The Response of the Macaque Tracheobronchial Epithelium to Acute Ozone Injury

A Quantitative Ultrastructural and Autoradiographic Study

DENNIS W. WILSON, DVM, PhD,
CHARLES G. PLOPPER, PhD, and
DONALD L. DUNGWORTH, BVSc, PhD

From the Departments of Veterinary Pathology and Anatomy, University of California, Davis, Davis, California

The tracheal epithelium of a variety of laboratory species is widely used as a model system in studies of epithelial biology and respiratory carcinogenesis. The purpose of this study was to evaluate the response of the tracheal epithelium to cytotoxic injury in a primate species that may have an epithelium more representative of that in man than smaller laboratory species. This study evaluated changes in the light-microscopic, surface, and ultrastructural appearance of the tracheobronchial epithelium of bonnet monkeys exposed for 3 or 7 days to 0.64 ppm ozone. Population densities, epithelial volumetric densities, and thymidine labeling indexes were determined for cells from posterior membranous and anterior cartilaginous trachea and mainstem bronchus. Ozone-induced epithelial changes were characterized by decreased numbers of ciliated cells, loss of cilia, and necrosis of ciliated cells. There were alterations in mucous (goblet) cell granules. There was an increase in extracellular space and focal epithelial stratification that was associated with increased numbers of small mucous granule cells and the presence of an epithelial cell type not seen in control animals (intermediate cells). There was an increase in cytoplasmic filaments and desmosomal attachments in basal cells, small mucous granule cells, and intermediate cells. Regional differences in lesion distribution were demonstrated by scanning electron microscopy. Longitudinal streaks of ciliary loss were evident in posterior membranous trachea, but ciliary loss in the ventral trachea was most prominent over the posterior border of the cartilaginous rings. The thymidine labeling index and numbers of necrotic ciliated cells were greater after 3 days than after 7 days of continuous exposure. Foci of stratification were often associated with increased numbers of labeled nuclei in the suprabasal region of the epithelium. The results of this study suggest that 1) small mucous granule cells and intermediate cells are important participants in the repair of chemically injured airway epithelium; 2) stratification and increased amounts of cytoplasmic filament bundles and desmosomal attachments, rather than being evidence of squamous metaplasia or dysplastic change, might be stereotypic responses of airway epithelium to injury; and 3) the ciliated cell population becomes less susceptible to ozone-induced necrosis with continuing exposure. (Am J Pathol 1984, 116:193-206)

THE TRACHEAL EPITHELIUM has been evaluated after injury by physical means, exposure to chemical carcinogens, and exposure to inhaled irritants. Physical injury generally denudes the surface of all or a portion of the epithelial population, resulting in repair by migration of adjacent cells or by division of remaining basal cells.[1] The response to chemical carcinogens varies from epithelial hypoplasia to hyperplasia and stratification with increased cytoplasmic filament bundles[2,3] and squamous metaplasia, dysplasia, and carcinoma.[4,5] Regions of carcinogen-exposed airway with morphologic changes have correspondingly increased rates of cell division.[2] Ciliated cells seem most susceptible to chemical injury. Ciliary damage has been described in rats exposed to 100% oxygen for 96 hours[6] and hamsters exposed to 200 ppm SO_2 for 6 weeks.[7] Short-term ozone exposure results in selective damage to ciliated cells, resulting in mitochondrial changes, loss of cilia, and increased ciliogenesis.[8-12] Scanning electron microscopic studies have revealed that these lesions occur in patches and streaks[12] and indicate that the posterior membranous

portion of the trachea is the most sensitive to ozone injury.[11] Stratification was reported due to subchronic (120 days) ozone exposure[13] and exposure to cigarette smoke.[14] Increased numbers of cytoplasmic filament bundles have also been reported in airway epithelium from dogs[14] and hamsters[15] in chronic cigarette smoke exposure studies.

It is therefore apparent that there are similarities in the responses of the tracheal epithelium to injury by a variety of carcinogenic and noncarcinogenic agents. Since it is difficult to separate the toxic from the carcinogenic effects of chemical carcinogens, it is important to understand the morphologic correlates and population dynamics of airway epithelial repair after injury by noncarcinogenic agents.

Many of the experimental pathobiologic studies of airway epithelium have been done with laboratory rodents. It is becoming apparent that there are major species differences in airway epithelial morphology.[16] We have recently described the ultrastructure of the normal tracheal epithelium of the bonnet monkey and suggested that primate airways may be a better model of human airways than those from most other laboratory species.[17] The purpose of the present study is to evaluate the response of primate airway epithelium to a primarily cytotoxic agent. The objectives are to describe and quantitate changes in morphologic features, distribution, and relative abundance of cell types in extrapulmonary airways of bonnet monkeys after relatively short-term exposure to high ambient concentrations of ozone and to localize and determine the rate of cell division in response to injury.

Materials and Methods

Animals

Nine adult male colony-born bonnet monkeys (*Macaca radiata*) between 4 and 9 years of age and weighing between 3.1 and 10.5 kg were used. The animals were shown to be free of clinical respiratory disease on the basis of physical examination, thoracic X-rays, and complete blood counts. They had been kept indoors and were placed in 4.2-cu m exposure chambers for 1 week prior to exposure. Three animals were in each group. One group was exposed to chemically and biologically filtered air, a second group to 0.64 ppm ozone continuously for 3 days, and a third group to 0.64 ppm ozone continuously for 7 days. Exposures were interrupted for 1 hour daily for maintenance of the animals. Ozone was generated by silent arc discharge and monitored each half-hour by a DASIBI UV ozone monitor calibrated by a DASIBI absolute ozone photometer. Concentrations of ozone

were recorded based on the ultraviolet photometric scale.

Following exposure, the monkeys were anesthetized with ketamine and injected intravenously with 1 miCi/kg of tritiated thymidine (specific activity 6.7 Ci/mmol) and kept in metabolism cages for 1 hour before euthanasia. The monkeys were killed by barbiturate injection and exsanguination via the abdominal aorta.

The trachea and lungs were immediately removed, the proximal trachea was cannulated, and the lungs and trachea were fixed by infusion with glutaraldehyde and paraformaldehyde diluted to 440 mOsm, pH 7.4.[19] After 1 hour of fixation, the proximal trachea was ligated, and the respiratory tract was immersed in fixative.

Tissue Selection and Processing

Consistent regions in the midlength of the trachea were selected by counting cartilage rings from the larynx. Rings 10-14 were prepared for scanning electron microscopy. They were divided longitudinally in thirds such that the posterior membranous portion and two lateral portions were processed. The tissues were dehydrated in a graded series of alcohols and amyl acetate, critical-point-dried with CO_2, and coated with gold by the use of a Denton Vacuum Sputter Coater. They were viewed on an ETEC scanning electron microscope. The fifteenth tracheal ring was cross-sectioned, and its caudal border was marked with a notch. Longitudinal sections of posterior membranous and anterior trachea were taken to include Rings 16-20. Similar longitudinal sections of the posterior and anterior right mainstem bronchus were made. These included the first four cartilage rings cranial to the division of the mainstem bronchus. These sections were dehydrated in a graded series of alcohol and propylene oxide and embedded in Epon-Araldite. The cranial border of Ring 15 was placed on the surface to be sectioned. Areas to be thin-sectioned were selected over cartilage rings in the anterior trachea and mainstem bronchus and were selected from the posterior membranous portion on the basis of good epithelial cross-sectional orientation. One-millimeter strips were cut from the large blocks and were reembedded in molds and thin-sectioned with a diamond knife on a Sorvall MT2-B microtome. Sections were mounted on Formvar-coated slotted copper grids and viewed with a Zeiss EM 10 microscope. Montages were prepared by photographing the entire section at ×1660 with photographic enlargement to approximately ×5000 on 8 × 10-inch prints. The magnification of each montage

was calibrated by photographing a grid with 600 bars/mm and printing it with the same enlargement.

Quantitation

Cell counts were based on counting all nuclear profiles on montages of electron micrographs of surface epithelium. Cells were identified on the basis of morphologic criteria given in the Results section or previously described.[18] The number of cells per millimeter airway was determined by the number of nuclear profiles per basement membrane length. Approximately 300 cells per montage were counted.

Stereologic data were derived by point counts with the use of a clear plastic square grid overlay with 63 grids 2.3 m on a side. Counting was done in two orientations, one parallel to and one at a 45-degree angle to the basement membrane. The grid was moved a randomly derived number of centimeters along the montage until the whole montage had been counted. A total of 400–600 points was tabulated for each montage. Points on the epithelium were divided into those falling on the nucleus (P_{nuc}) and cytoplasm (P_{cyt}) of each cell type, as well as those on extracellular space ($P_{extracell}$). Volume densities were determined with the following formulas[19]:

$$V_{nuc}/V_{cell} = P_{nuc}/P_{cell} \text{ (nuc + cytoplasm)}$$
$$V_{cell}/V_{epith} = P_{cell}/P_{epith}$$
$$V_{extracell}/V_{epith} = P_{extracell}/P_{epith}$$

where P_x is the total number of points counted as overlying that structure (x) in the montage and P_{epith} is the total number of points counted in the montage. Cross-sectional areas of nuclear profiles were determined by planimetry with the use of a Zeiss MOP 3 image analyzer. Nuclear profile area distributions were based on the frequency of profiles occurring in groups defined by 0.25×10^{-5}-sq mm increments. Comparison between groups were evaluated by both a one-way analysis of variance and a two-tailed t test.[20]

Autoradiography

One-micron epoxy sections on glass slides were further polymerized by heating at 60 C for 12 hours. Slides were dipped in Ilford L4 photographic emulsion mixed 50:50 with water at 40 C. They were allowed to dry, placed in light-tight boxes containing desiccant, and kept at 4 C for 4 weeks. Autoradiographs were developed in microdiol X, fixed with 15% sodium thiosulfate, and stained with toluidine blue. A labeling index was determined by counting 1000 cells per section at ×1000 and determining the number of labeled cells/100 nuclei counted. Cells were considered labeled if there were five or more silver grains directly above the nucleus.

Results

Surface Morphology

The major change in surface structures due to ozone exposure was the loss of ciliated cells and the presence of cells with a microvillar surface or cells with attenuated cilia (Figures 2 and 3) when compared to control animals (Figure 1). As previously reported,[17] there are regional differences in the surface morphology of the primate extrapulmonary airways. The major difference is the presence of longitudinal linear arrays of secretory cells on the posterior portion of the trachea that are not present on the anterior portion. In the animals exposed for 3 days to 0.64 ppm ozone, there were longitudinal streaks of ciliary loss on the posterior portion of the trachea (Figure 5) but only patchy regions on the anterior surface (Figures 7 and 8). Ciliated cells adjacent to the linear secretory cell arrays seemed relatively spared in comparison with those in regions with fewer secretory cells (Figure 6). In animals exposed for 7 days, the affected regions on the posterior portion had become more generalized, whereas on the anterior surface distinct regions of ciliary loss were apparent in epithelium over the posterior border of cartilage rings and in intercartilaginous regions (Figures 9 and 10). Although it was difficult to distinguish among nonciliated cells in the ozone-exposed animals, three general types were present (Figure 3). One had relatively long microvilli and a slightly dome-shaped surface. The microvilli on these cells were very similar to those on ciliated cells with attenuated cilia. The second type was also slightly dome-shaped and had shorter but irregular length microvilli. The third cell surface type was a flat polygonal cell with slightly raised borders and abundant short microvilli of even length. Both of the latter two cells had superficial cavitations and small aggregates of amorphous material on their surface that was interpreted to represent discharging mucus (Figure 4).

Ultrastructural Changes

By transmission electron microscopy, two types of damaged ciliated cells could be discerned. There were regions where most ciliated cells did not differ from controls. In other areas there was a high frequency of ciliated cells that had basal bodies but only short or absent cilia. In some of these cells there were aggregates of irregularly oriented basal bodies in the apical
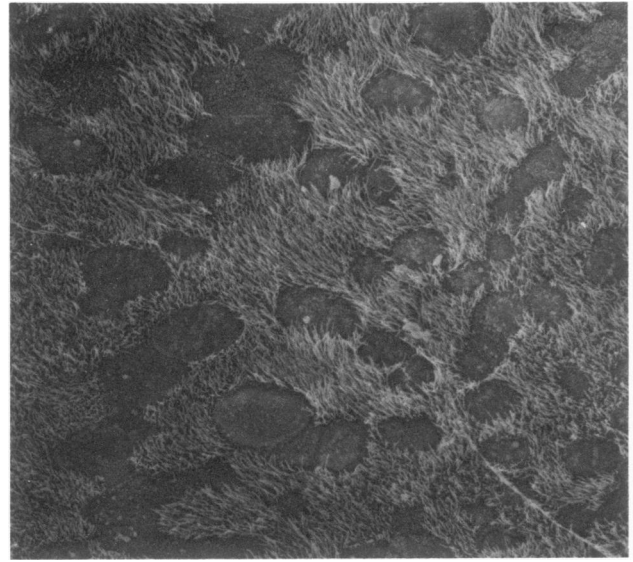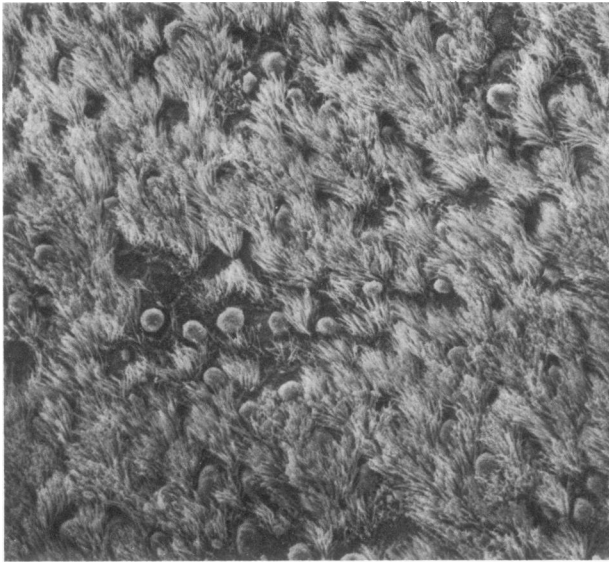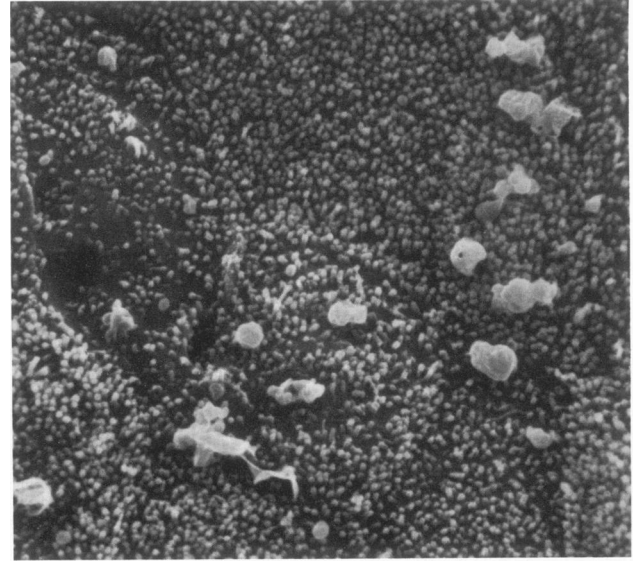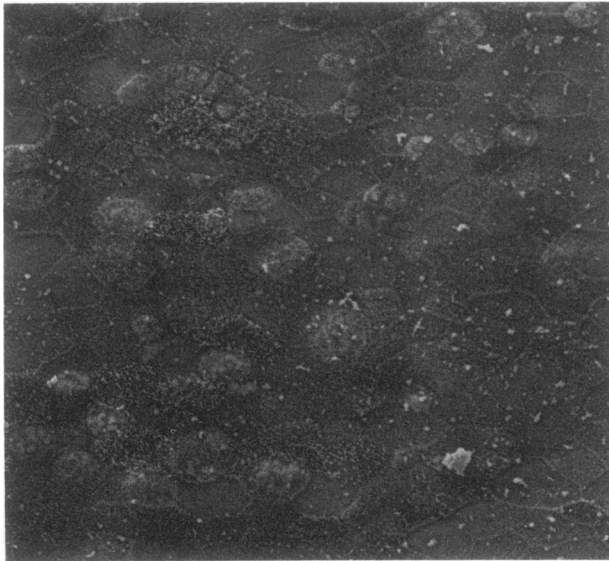
Figure 1—Surface of tracheal epithelium from a bonnet monkey exposed to filtered air for 3 days. Many secretory cells have protrusions of apical cytoplasm into the lumen. (×700)   **Figure 2**—Surface of tracheal epithelium from a bonnet monkey exposed for 3 days to 0.64 ppm ozone. Cilia are sparse and shortened. There are numerous flat microvillar surfaced cells in regions of ciliary loss. (×700)   **Figure 3**—Types of nonciliated cells in tracheal epithelium of a bonnet monkey exposed to 0.64 ppm ozone for 7 days. There are cells with slightly raised surface with long microvilli, cells with raised surface and short microvilli, and cells with a flat polygonal surface, short microvilli, and raised borders. (×700)   **Figure 4**—Higher magnification of flat polygonal cells. These cells most likely represent intermediate cells. Small caveoli are present on the surface, and there are flecks of material that probably represent secretory product above them. (×5800)

Figure 5—Low magnification of the surface of the posterior membranous trachea from a bonnet monkey exposed for 3 days to 0.64 ppm ozone. The cranial end is marked with a notch. Note the longitudinal streaks of ciliary loss indicated by the lighter gray regions. The *box* indicates the location of Figure 6. (×20)   **Figure 6**—Higher magnification of a region from Figure 5 showing the junction of a region of ciliary loss (A) with one where cilia are relatively spared (B). A normal longitudinal row of secretory cells (*arrow*) has relatively normal ciliated cells on either side. The top of the picture is cranial. (×800)   **Figure 7**—Surface of anterior trachea from a bonnet monkey exposed for 3 days to 0.64 ppm ozone. Ciliary loss (A and **Figure 8A**) occurs in irregularly oriented patches surrounded by regions of relatively normal ciliated cells (B and **Figure 8B**).   **Figure 8A**—Ciliary loss in region A from Figure 7.   **B**—Relatively normal cilia from region B in Figure 7. (×650)   **Figure 9**—Ventral trachea from a bonnet monkey exposed to 0.64 ppm ozone for 7 days. The cranial border is at the *top* of the picture. Regions of loss of cilia (A and **Figure 10A**) overlie predominantly the posterior border of the cartilage and intercartilage regions, while other areas appear unaffected (B and **Figure 10B**) (×20)   **Figure 10A**—Ciliary loss in region A from Figure 9. Note the prominent flat polygonal cells compared with Figure 8A.   **B**—Relatively normal cilia from region B in Figure 9. (×650)
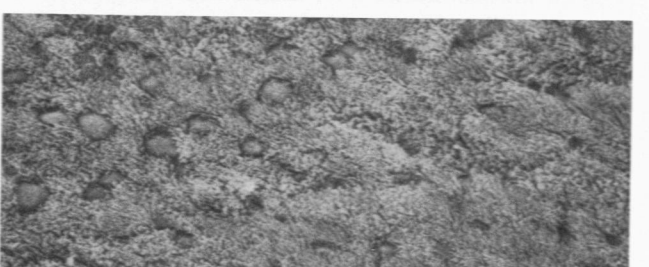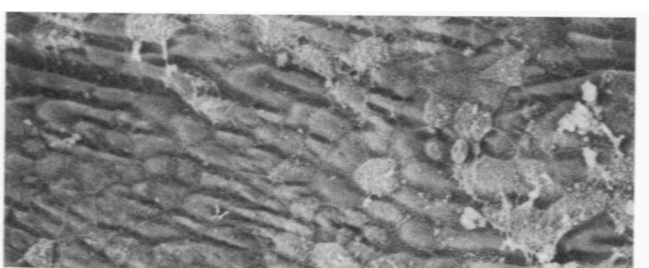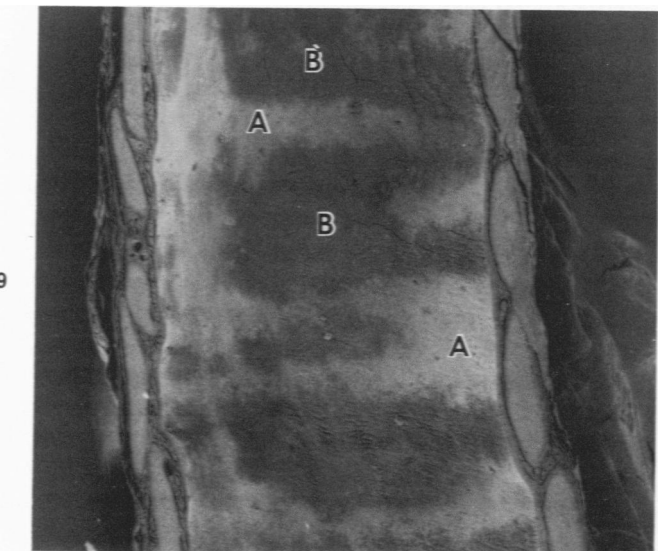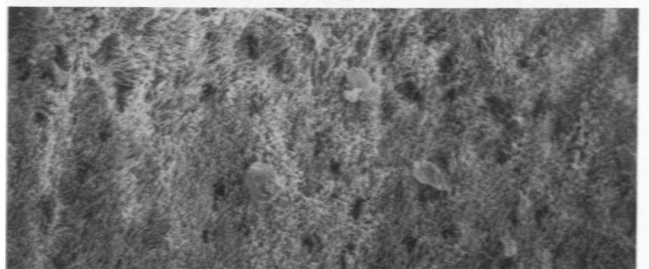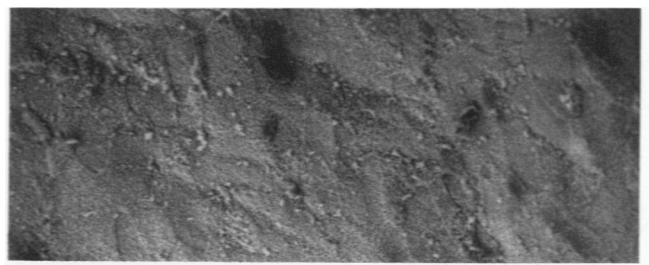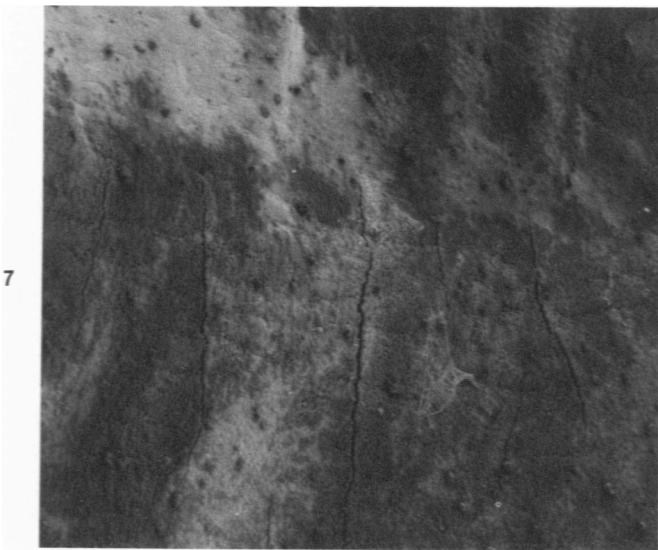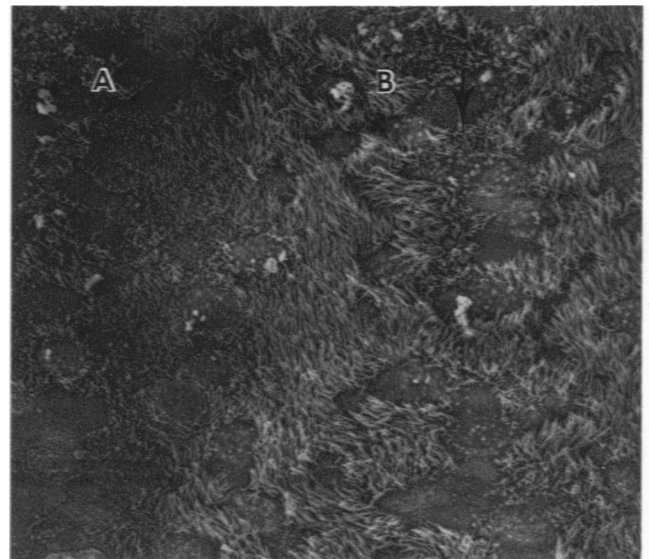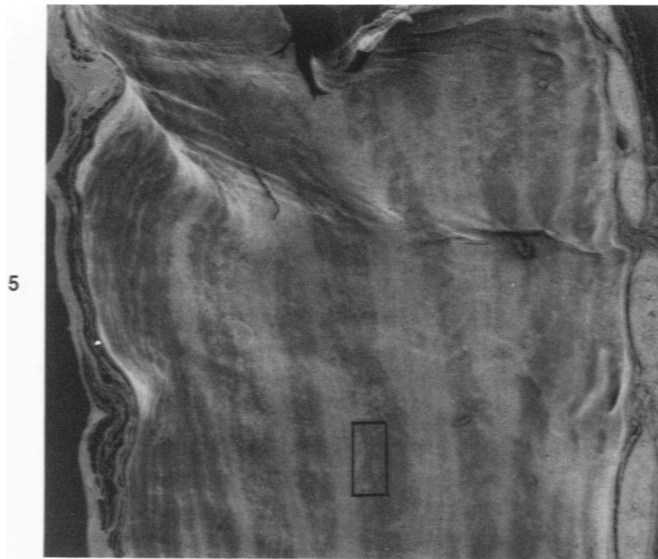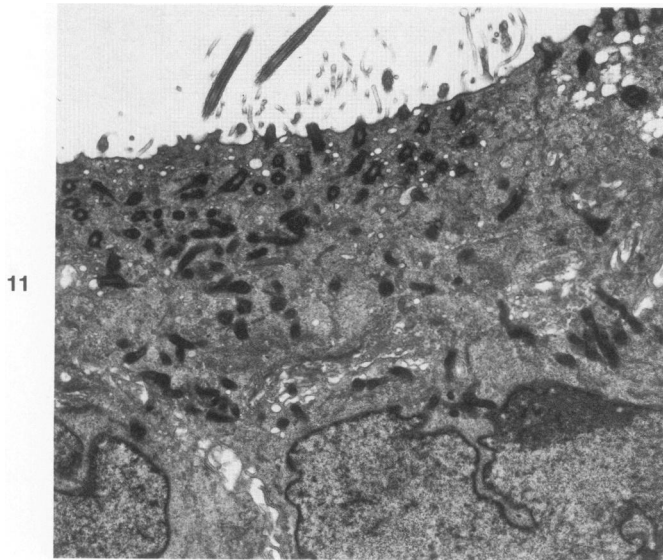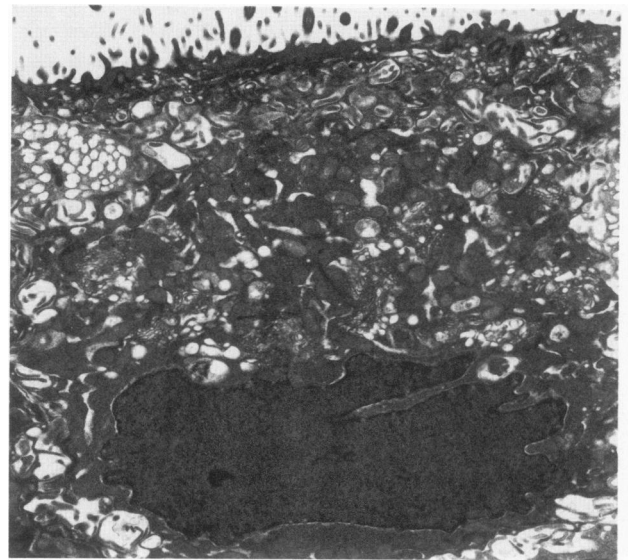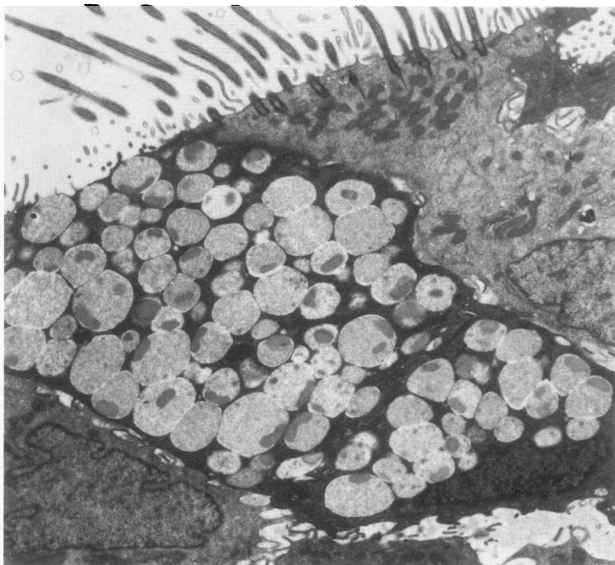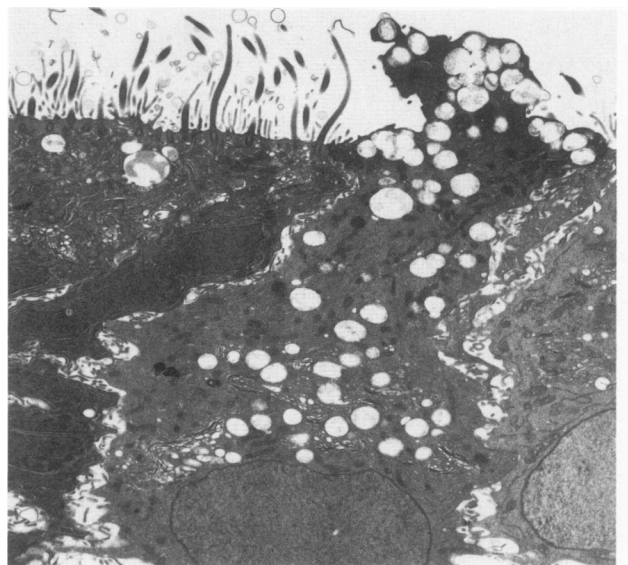
Figure 11—Ciliated cell with short cilia and aggregates of irregularly oriented basal bodies in apical cytoplasm. (×6412)   **Figure 12**—Necrotic ciliated cell with electron-dense cytoplasm and nucleus and dilated endoplasmic reticulum. (×6412)   **Figure 13**—Mucous goblet cell from normal animal. This cell has granules with prominent electron-dense cores and flocculent peripheral material. Granules fill the majority of the cytoplasm. Compare this with the mucous cell from the ozone-exposed animal in Figure 14. (×5202)   **Figure 14**—Mucous cell from ozone exposed animal. The nucleus is less electron dense and less angular than normal (Figure 10). The granules lack central cores and are a much smaller proportion of the cytoplasm than normal mucous cells. (×3825)

cytoplasm (Figure 11). The second type of damaged ciliated cell was randomly distributed and characterized by extremely electron-dense staining, condensed mitochondria, a shrunken dense angular nucleus, a dilated cytocavitary network (Figure 12). These cells were interpreted as having undergone irreversible changes. Some had cilia of regular length, and others had short, attenuated cilia and occasionally had evidence of ciliogenesis. They appeared randomly dispersed among more normal ciliated cells. Intraepithelial inflammatory cells, usually polymorphonuclear leukocytes, were occasionally seen in both control and ozone-exposed animals.

Decreased density and altered morphology of secre-

tory granules were the most consistent changes in mucous cells. Mucous granules were more irregularly sized than controls. The granules in general appeared smaller and contained only filamentous to granular secretory material. The biphasic nature of the control mucous granules was usually not evident in ozone-exposed animals (Figure 14). Many more mucous cells in the ozone-exposed animals had relatively few mucous granules dispersed in a relatively large amount of cytoplasm. Nuclei of mucous cells in ozone-exposed animals also appeared larger, less angular, and less electron-dense, with relatively more euchromatin (Figure 14).

Small mucous granule cells (SMG) were more

prominent in ozone-exposed animals than in controls. They had more abundant cytoplasm with a greater number of specific granules (Figure 15). While occasional bundles of filamentous material were present in controls, stratified SMG cells from ozone-exposed animals had markedly increased amounts of filamentous material arranged in irregularly oriented bundles that were occasionally associated with desmosomes. Desmosomal attachments between SMG cells and adjacent cells were much more frequent in ozone-exposed animals (Figure 16). Similar increases in filament bundles and desmosomal attachments were evident in basal cells.

A cell type was present in ozone-exposed animals that was not seen in controls (Figure 17). These cells had a microvillar surface that frequently extended over adjacent cells (Figure 21). The surface microvilli appeared to be of even length. The body of these cells was pyramidal or cone-shaped with narrow basal cytoplasm that did not appear to extend beyond the mid region of the epithelium. The nucleus varied but was generally round, with a smooth surface and dispersed chromatin. The cytoplasm of these cells had frequent filament bundles, granular endoplasmic reticulum, a perinuclear Golgi apparatus, and mitochondria in moderate numbers. They were attached at the apex to adjacent cells by typical junctional complexes. The apical cytoplasm frequently contained secretory granules containing lightly electron-dense fibrillar material. These apical granules were often arranged in a row immediately beneath the surface but were irregularly arranged in some cells. Some of these cells had sufficient numbers of granules to resemble mucous cells (Figure 18). In others, fibrogranular aggregates and basal body division was evident, suggesting differentiation toward ciliated cells (Figures 19 and 20). Because they showed early features of two mature cell types, these cells were called intermediate cells.

In addition to the changes in cellular morphology, some changes in the epithelium as a whole were noted. There was an apparent increase in extracellular space. There were numerous foci where the epithelium appeared truly stratified (Figure 21). Sectioning blocks at varying angles did not alter the stratified appearance. These regions generally had a surface lined by intermediate cells. The midportions of the epithelium contained primarily SMG cells, whereas the base of the epithelium consisted of both basal and SMG cells. These regions of stratification had cells with the most prominent cytoplasmic filaments and desmosomal attachments.

Morphometric Data

The following morphometric parameters were de-

termined: volume percentage of each cell type within the total epithelial volume (Figure 22a–c), population density (percent) of each cell type (Figure 23a–c), volume percentage of nucleus/total cell for each cell type (Figure 24a–c), and median nuclear cross-sectional area for each cell type (Figure 25a–c). After 3 days of exposure there were significant decreases in both the population percentage and volumetric density of ciliated cells in the trachea. The extracellular space was also significantly increased. By 7 days the population density and volumetric density of ciliated cells had returned toward normal. Similarly, the numbers and volume density of intermediate cells and necrotic ciliated cells were greatest at 3 days and less at 7 days. Numbers of SMG cells remained high at 7 days, and there was still a significant increase in their volumetric density. Changes in the mainstem bronchus were similar but less pronounced and were not statistically significant. The median nuclear cross-sectional area of mucous cells was significantly increased at both time intervals in the anterior trachea only.

Autoradiography

Only cells with basal nuclei were labeled in control animals. It was not generally possible to distinguish between basal cells and SMG cells in the autoradiographs, and so it was not known whether the control labeled cells were basal or SMG cells. In ozone-exposed animals, both basal and suprabasal nuclei were labeled. Some labeled cells could be seen to have cytoplasmic mucous granules (Figure 26). The calculated labeling index is presented in Table 1. The labeling index was increased by a factor of 1.5–5 times control at 3 days but had only a small and statistically nonsignificant increase at 7 days. A wide range of variability in labeling index was evident. This occurred because the labeling was nonuniform in that there were foci which contained a large percentage of labeled cells alternating with areas with a relatively low labeling frequency. Generally the highly labeled areas were associated with the more severe lesions. The highest frequency and greatest percentage of

Table 1 — Labeling Index (Percent Labeled Nuclei) for Extrapulmonary Airways From Bonnet Monkeys Exposed for 0, 3, or 7 Days to 0.64 ppm Ozone

	Control	3 days	7 days
Anterior trachea	0.7 ± 0.2	3.4 ± 1.3	1.6 ± 1.0
Posterior trachea	0.8 ± 0.15	1.1 ± 0.3	0.6 ± 0.3
Anterior mainstem bronchus	0.8 ± 0.2	3.0 ± 2.7	0.7 ± 0.5
Posterior mainstem bronchus	0.5 ± 0.4	3.1 ± 2.0	3.3 ± 3.5
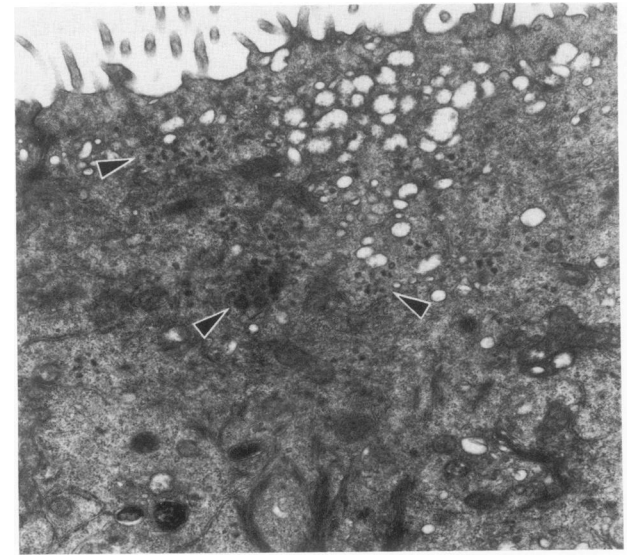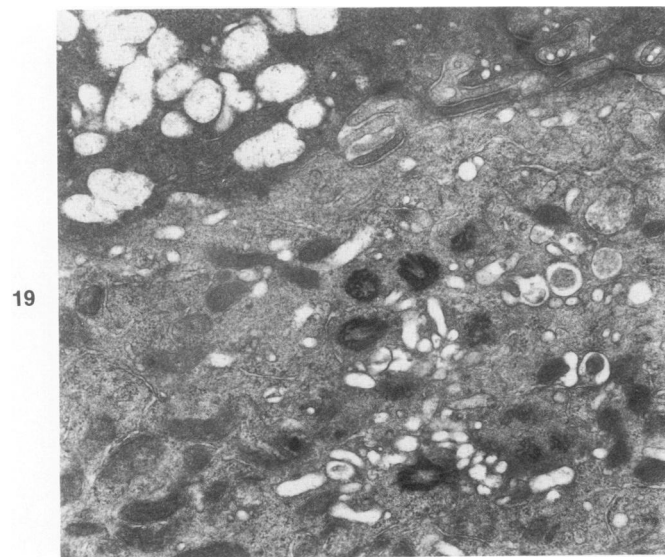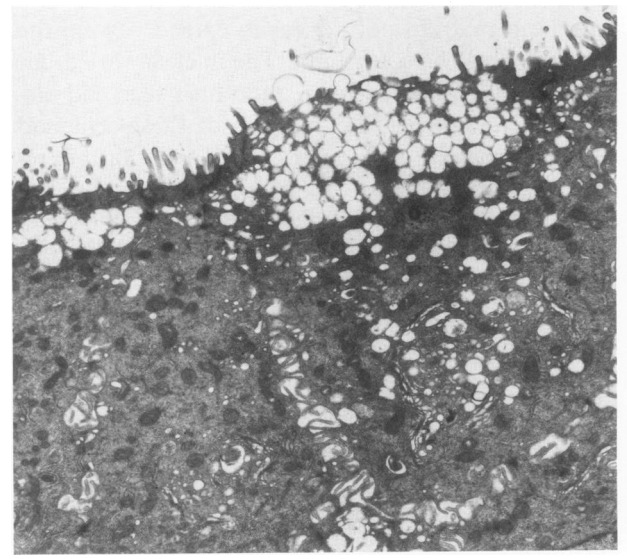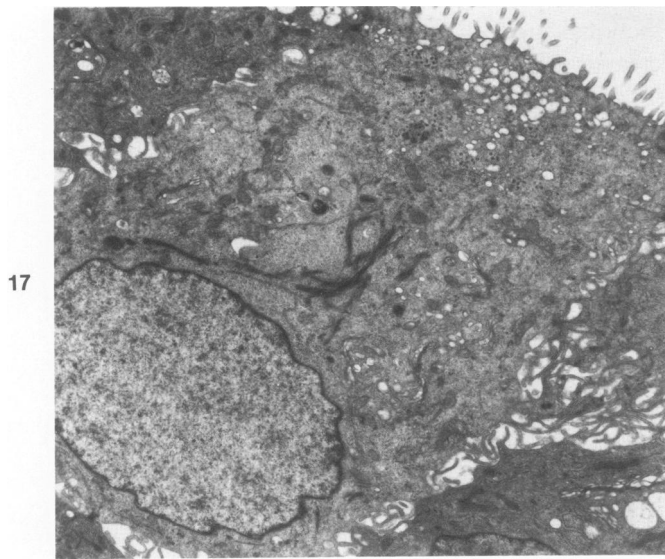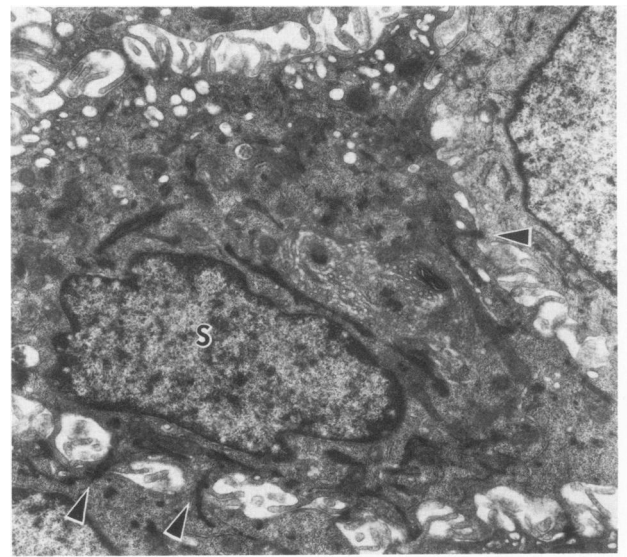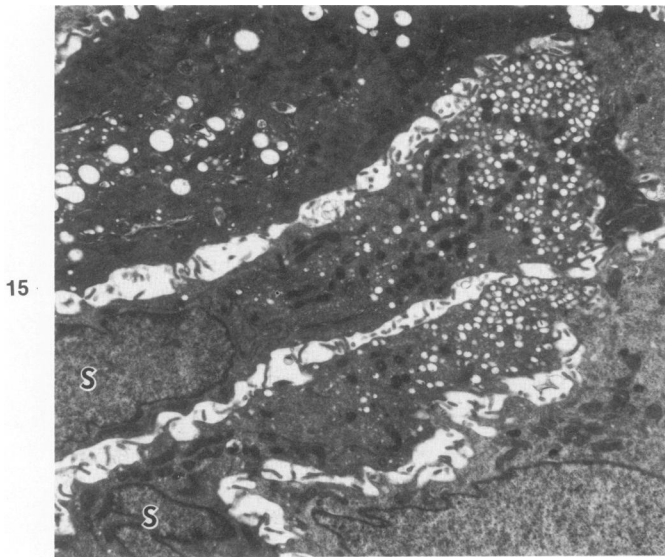
labeled suprabasal cells occurred in the regions of stratification (Figure 27).

Discussion

We find several changes in the extrapulmonary airway epithelium after a 3-day exposure to ozone that are similar to those described previously with longer exposures to ozone or exposure to carcinogenic agents. Continuous exposure to 0.64 ppm for 3 days results in significant ciliated cell necrosis, an altered appearance to mucus-secreting cells, and an increase in extracellular space. Repair of this injury involves hypertrophy and hyperplasia of SMG cells and proliferation of a cell type not found in normal airway epithelium, the intermediate cell. Associated with this process is an increase in cell-to-cell attachments (desmosomes) between basal, SMG, and intermediate cells and an increased number of cytoplasmic filament bundles. Where the proliferation of SMG cells and intermediate cells is most pronounced, there is markedly increased cell labeling with tritiated thymidine. It is likely that these changes represent a stereotyped response of the airway epithelium to acute chemical injury.

Previous observations[9-11] showed that ozone exposure results in ciliated cell damage in the extrapulmonary airways. Results of this study suggest that ciliary loss is a reversible cellular change not necessarily linked to cell necrosis. These cells probably represent mature cells that are regenerating lost cilia. Many otherwise unaltered ciliated cells with short fragmented cilia and properly oriented apical basal bodies had aggregates of proliferating basal bodies in their apical cytoplasm. Some dark-staining cells with marked separation of cytoplasm from organelle membranes had evidence of ciliogenesis, and other dark cells had complete nonfragmented cilia. These cells were interpreted to have undergone irreversible change that was independent of the presence or absence of ciliary loss. Similarly, some dark necrotic cells had evidence of ciliogenesis, and others had complete nonfragmented cilia.

Changes in the morphology of mucous goblet cells associated with ozone exposure have not been previously documented. In addition to altered granule morphology, there was a trend toward lower volume density of mucous cells but no change in population density. This suggests that the mucous cells are smaller in ozone-exposed animals, probably because of decreased numbers of secretory granules. Changes in mucous cells may represent increased mucus secretion, decreased or altered mucus synthesis, or immaturity of newly formed mucous cells. The last possibility seems unlikely, because a majority of mucous cells had fewer, less well organized mucous granules; whereas mucous cell necrosis was not seen, and mucous cell division was infrequent. Although decreased incorporation of mucus precursors reported in tracheal explants from rats exposed to ozone for 1 week[21] implies that there is less secretion, the relative paucity of goblet cells with cytoplasm filled with granules in ozone-exposed animals suggests that mucous discharge must have occurred at some point.

Studies in other species suggest that secretory cell division may be important in the repair of injured tracheobronchial[22,23] and bronchiolar[24] epithelium. An apparent but not absolute increase in secretory cells in injured hamster trachea was accounted for by accumulation of secretory granules in preexisting cells.[25] Since SMG cells increased with regard to the relative percentage of the population on the basis of nuclear profile counts as well as with regard to the volume percentage of the epithelium, this increase was interpreted to be due to cell proliferation and not to accumulation of secretory product. While the function(s) of the SMG cell are unknown, their increase in ozone-exposed animals may reflect a role as a precursor cell in the repair process and/or an increased functional activity. A similar increase in "special type" cells which have morphologic characteristics similar to those of the SMG cells was reported for dogs exposed to cigarette smoke.[14] Although it is not always possible to distinguish SMG cell and basal cell nuclei on autoradiographs, the presence of large numbers of labeled nuclei in the suprabasal area in regions of stratification and the presence of large numbers of SMG cells in similar regions on electron micrographs suggest that these cells have an important proliferative function. Ultrastructural autoradiography or cell kinetic studies will be necessary to prove this hypothesis.

Figure 15 — Abundant cytoplasm containing large numbers of vesicles in small mucous granule cells (S) from ozone-exposed animals. (× 5186)   Figure 16 — Large amounts of cytoplasmic filament bundles are present in these stratified small mucous granule cells (S) from ozone-exposed animals. Notice the prominent desmosomal attachments (arrow) to adjacent cells. (× 8882)   Figure 17 — Intermediate cell from an ozone-exposed animal. Notice the numerous short surface microvilli and abundant cytoplasmic filament bundles. (× 4972)   Figure 18 — Aggregates of vesicles near the apex of an intermediate cell, suggesting differentiation toward a mucous cell. (× 6600)   Figure 19 — Aggregates of basal bodies in apical cytoplasm of an intermediate cell, suggesting differentiation toward a ciliated cell. (× 14400)   Figure 20 — Fibrogranular aggregates (fibrosomes and deuterosomes, arrows) in the apical portion of an intermediate cell, suggesting differentiation toward a ciliated cell. (× 11,853)
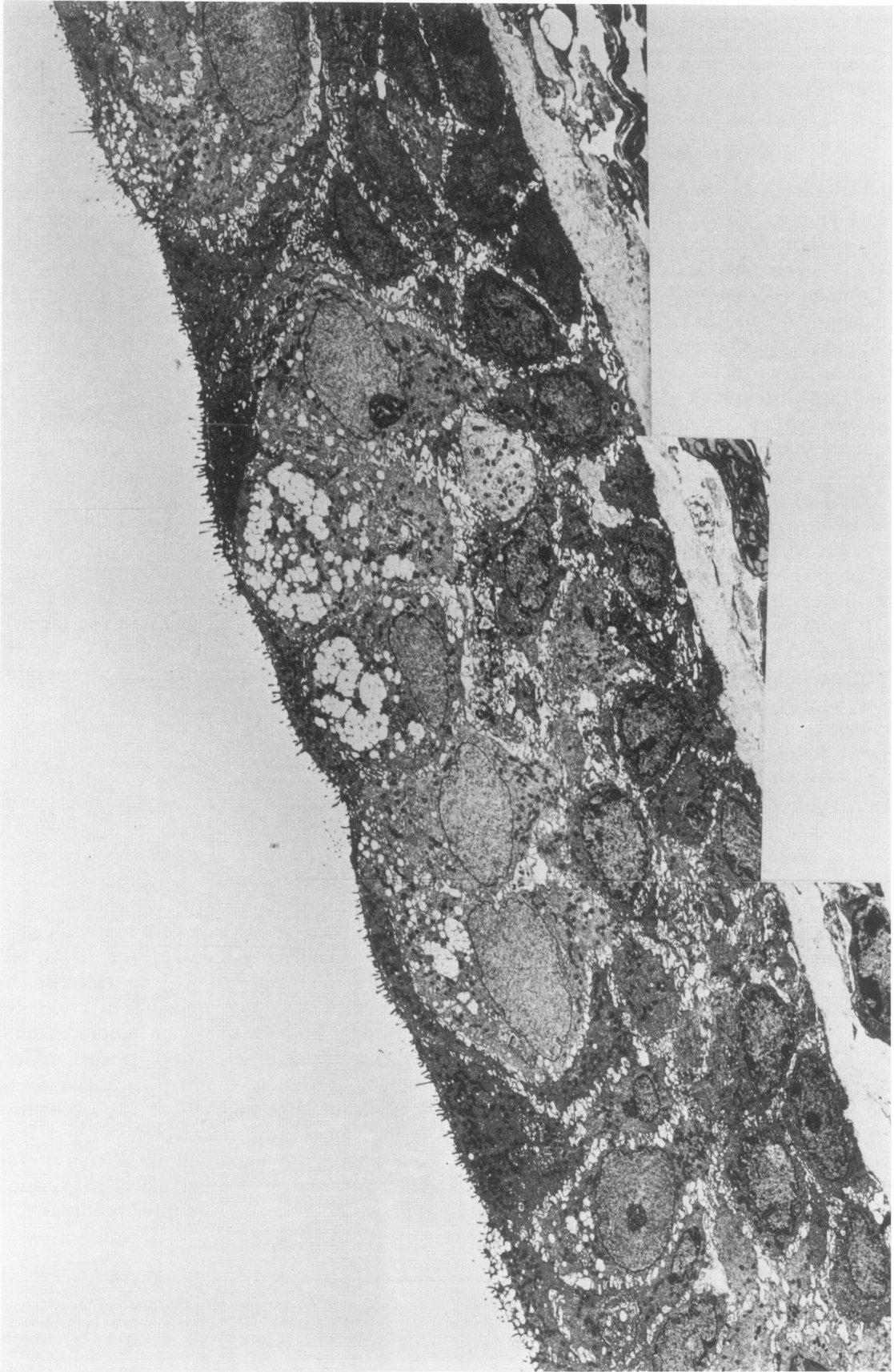
Figure 21 — Montage of a region of stratification in ozone-injured tracheal epithelium. Intermediate cells line the surface and have extensions of apical cytoplasm, which cover the surface of adjacent cells. Small mucous granule cells are prominent in the middle layer of the epithelium overlying the basal cell layer. (×2519)

VOLUME PERCENTAGE OF TOTAL EPITHELIUM IN THE POSTERIOR TRACHEA OF BONNET MONKEYS EXPOSED TO 0.64ppm OZONE

A

VOLUME PERCENTAGE OF TOTAL EPITHELIUM IN THE ANTERIOR TRACHEA OF BONNET MONKEYS EXPOSED TO 0.64ppm OZONE

B

VOLUME PERCENTAGE OF TOTAL EPITHELIUM IN THE MAINSTEM BRONCHUS OF BONNET MONKEYS EXPOSED TO 0.64ppm OZONE

C
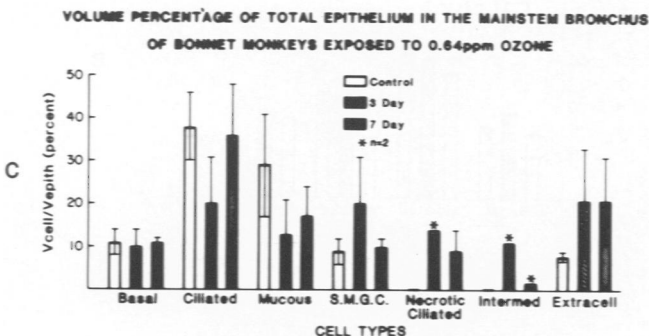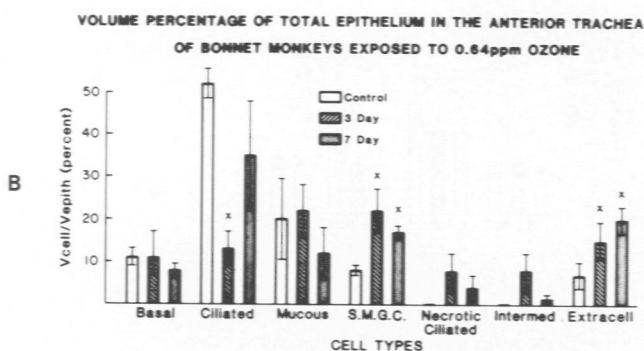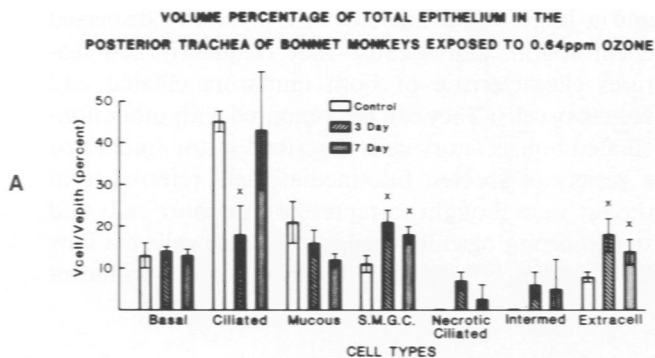
Figure 22 — Volume density of cells in the total epithelium of airways from bonnet monkeys exposed for 3 or 7 days to 0.64 ppm ozone. A — Posterior membranous trachea.   B — Anterior cartilaginous trachea.   C — Mainstem bronchus. X indicates P < 0.05.

Repair of oxidant-induced injury appears to occur by proliferation of basal and suprabasal (SMG and goblet) cells, resulting in epithelial stratification. Some superficial thymidine-labeled cells appear to lack contact with the basement membrane. These cells have a large luminal surface that covers adjacent injured epithelium and in many instances have secretory droplets, implying a secretory function. These cells apparently can then differentiate into either secretory (goblet) cells, as evidenced by the presence of

aggregates of secretory granules in their cytoplasm, or into ciliated cells, as evidenced by the presence of basal body precursors and aggregates of basal bodies in the apical cytoplasm. Since the superficial cells are often associated with regions overlying hyperplasia of SMG cells, they may be products of either SMG cell or goblet cell division. Repair of severe damage in the trachea and bronchi therefore has some similarities to epithelial repair in smaller airways, where the predominant progenitor cell is also a nonciliated secretory cell, the Clara cell.[24,27]

POPULATION DENSITY (percent) OF CELLS IN THE POSTERIOR TRACHEA OF BONNET MONKEYS EXPOSED TO 0.64ppm OZONE

A

POPULATION DENSITY (percent) OF CELLS IN THE ANTERIOR TRACHEA OF BONNET MONKEYS EXPOSED TO 0.64ppm OZONE

B

POPULATION DENSITY (percent) OF CELLS IN THE MAINSTEM BRONCHUS OF BONNET MONKEYS EXPOSED TO 0.64ppm OZONE

C
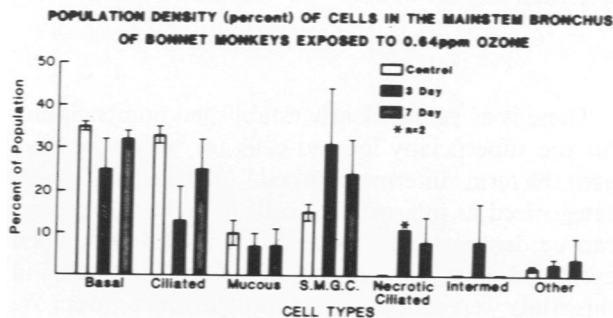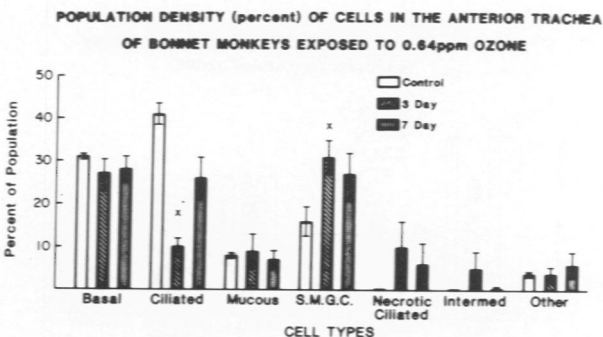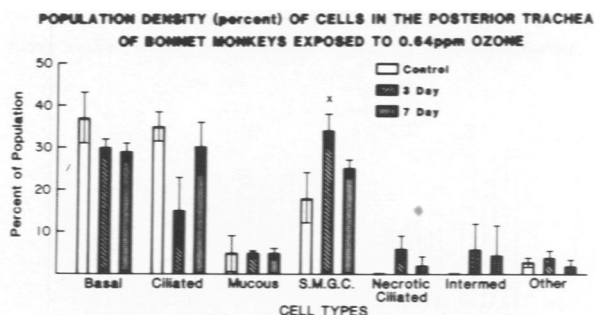
Figure 23 — Population density based on counts of nuclear profiles of cells in airway epithelium of bonnet monkeys exposed for 3 or 7 days to 0.64 ppm ozone.   A — Posterior membranous trachea. B — Anterior cartilaginous trachea.   C — Mainstem bronchus. X indicates P < 0.05.

VOLUME PERCENT NUCLEUS: TOTAL CELL IN THE
POSTERIOR TRACHEA OF BONNET MONKEYS EXPOSED TO 0.64ppm OZONE

VOLUME PERCENT NUCLEUS: TOTAL CELL IN THE
ANTERIOR TRACHEA OF BONNET MONKEYS EXPOSED TO 0.64ppm OZONE

VOLUME PERCENT NUCLEUS: TOTAL CELL IN
IN THE MAINSTEM BRONCHUS OF BONNET MONKEYS
EXPOSED TO 0.64ppm OZONE
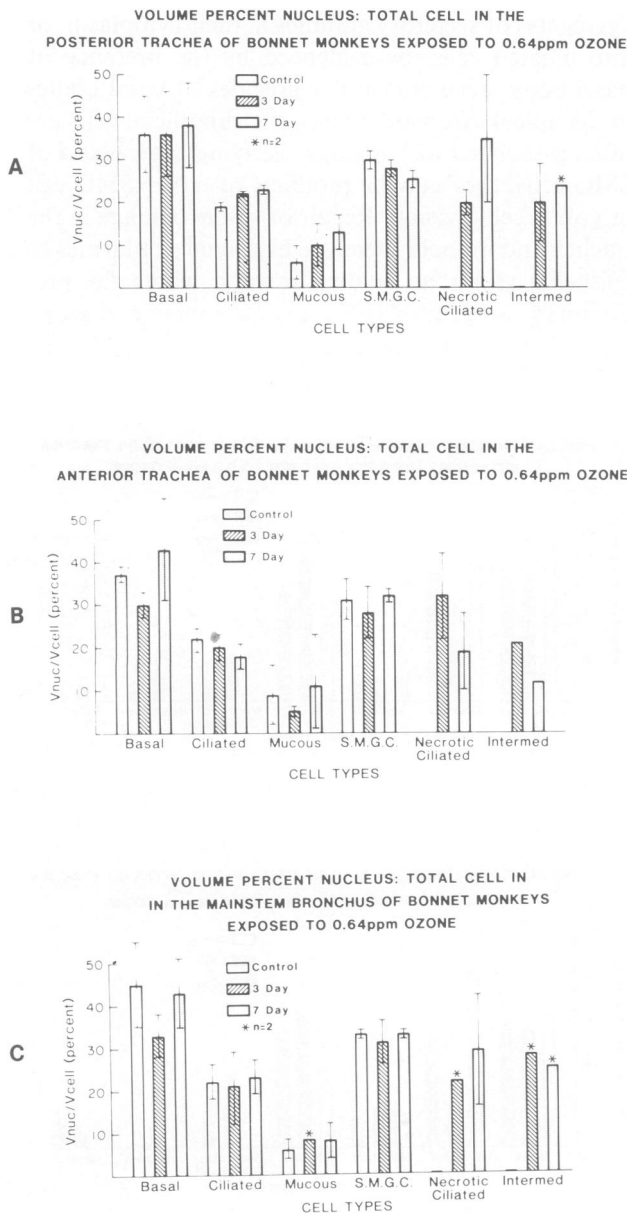
Figure 24 — Volume density of nucleus in the total cell volume from cell types in airways from bonnet monkeys exposed for 3 or 7 days to 0.64 ppm ozone.   A — Posterior membranous trachea.   B — Anterior cartilaginous trachea.   C — Mainstem bronchus. X indicates $P < 0.05$.

and a large round nucleus with primarily dispersed euchromatin, and because they frequently had features characteristic of both immature ciliated and secretory cells. They can be compared with other nonciliated nonsecretory cells described in the trachea of a variety of species. Intermediate cells referred to in the rat were thought to represent immature cells and were morphologically similar to ciliated cells but lack basal bodies.[28,29] Indifferent cells with electron-lucent

MEDIAN NUCLEAR CROSS SECTIONAL AREA
IN THE POSTERIOR TRACHEA OF
BONNET MONKEYS EXPOSED TO 0.64ppm OZONE

MEDIAN NUCLEAR CROSS SECTIONAL AREA
IN THE ANTERIOR TRACHEA OF BONNET MONKEYS
EXPOSED TO 0.64ppm OZONE

MEDIAN NUCLEAR CROSS SECTIONAL AREA
IN THE MAINSTEM BRONCHUS OF
BONNET MONKEYS EXPOSED TO 0.64ppm OZONE
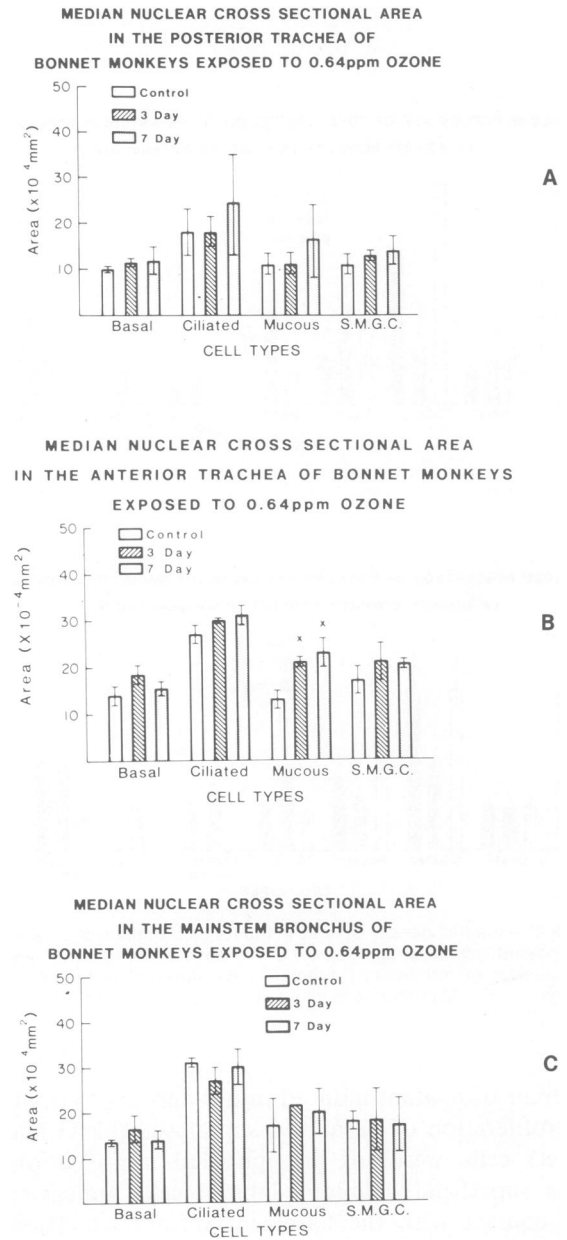
Figure 25 — Median nuclear cross-sectional area of cell types from airway epithelium of bonnet monkeys exposed for 3 or 7 days to 0.64 ppm ozone.   A — Posterior membranous trachea.   B — Anterior cartilaginous trachea.   C — Mainstem bronchus. X indicates $P < 0.05$.

There is as yet no clearly established nomenclature for the superficially located cells for which we have used the term "intermediate cell." Whereas many cells categorized as intermediate cells by light microscopy can be demonstrated to be differentiated cells when examined ultrastructurally,[26] the intermediate cells in this study were an ultrastructurally distinct group. We prefer the designation "intermediate cell" because they appeared morphologically immature, as characterized by a paucity of organelles in the cytoplasm

Figure 26 — Autoradiograph of tracheal epithelium of a bonnet monkey exposed for 3 days to 0.64 ppm ozone and given tritiated thymidine. Notice the subrabasal labeled nucleus in a cell containing cytoplasmic mucous granules (arrow). (×1066)

Figure 27 — Autoradiograph of tracheal epithelium of a bonnet monkey exposed for 3 days to 0.64 ppm ozone and given tritiated thymidine. Notice the large proportion of labeled suprabasal nuclei in this region of stratification. (×575)
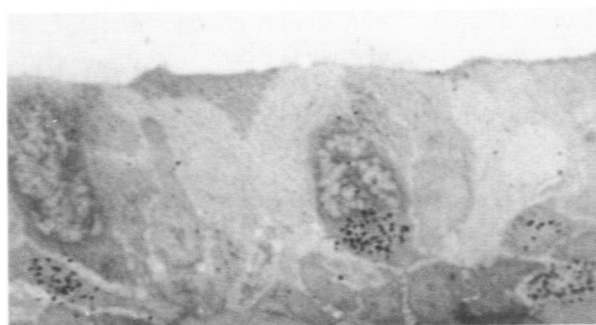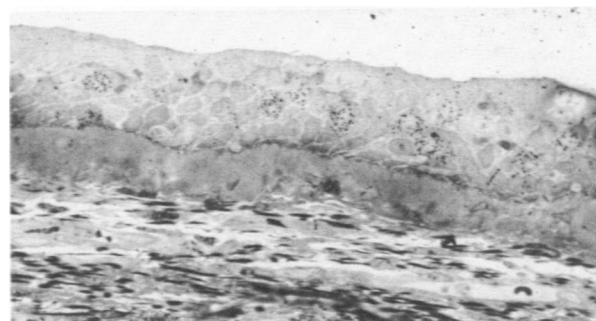
cytoplasm containing scant organelles were described as a rare cell type in human bronchi.[30] These cells occasionally had evidence of differentiation toward secretory or ciliated cells. The intermediate cells described in this study differ from those previously mentioned in that they are primarily surface-oriented and do not appear to extend to the basement membrane. They appear to have a structural function, because the flat microvillar surface extends over adjacent cells. It seems likely that the flat polygonal cells with raised borders seen on scanning electron microscopy are intermediate cells covering regions of injured epithelium. These cells, in addition to serving as precursor cells for a more differentiated epithelium, may serve a protective function by rapidly restoring mucosal integrity to an injured epithelium.

The alteration in epithelial morphology resulting from ozone exposure most resembles the recently described epidermoid metaplasia in the hamster trachea damaged by physical injury.[31] These authors also present evidence that this change results from division of secretory cells and that it rapidly resolves by differentiation toward normal mucociliary epithelium. The increased numbers of desmosomal attachments and intermediate filament bundles seen in this study suggest that this also is a response to injury and not an altered state of differentiation. Since the process we have described appears to be a transient stage of the rapidly reversible normal repair process and not a replacement of the one differentiated cell type

by an altered but mature cell type, we believe it is misleading to label it as a metaplastic change.

Results of this study also have applications to ozone toxicology. The pathogenesis of the apparent regional differences in lesion orientation is uncertain. It seems likely that the longitudinal streaks of ciliary loss in the posterior trachea are somehow related to the presence of goblet cell and glandular lines which are present in that region. The location of more intense lesions in the anterior trachea at the caudal border of cartilage rings cannot be explained by local differences in mucus secretion.

While ciliary loss apparent by scanning electron microscopy appeared more extensive in the posterior membranous trachea, morphometric evaluation by transmission electron microscopy did not reveal differences in numbers of necrotic ciliated cells, intermediate cells, or amount of extracellular space between posterior and anterior trachea. Morphometric data did indicate, however, that the mainstem bronchus was less affected by ozone exposure.

Results of morphometric determinations and autoradiography in this study suggest that the epithelium was more altered at 3 days and had less alteration after 7 days of exposure. Reasons for this are still unclear. It is possible that relatively young cells are metabolically more resistant to the oxidant than the more mature cells which preceded them. Biochemical changes such as induction of superoxide dismutase systems have been reported in lungs of oxygen-

exposed animals,[32] and similar changes may protect tracheobronchial epithelial cells from further damage. The decreased damage may be evidence of early adaptation to continuous oxidant exposure. In a recently completed study, changes were minimal in bronchial ciliated cells from bonnet monkeys exposed for 1 year to 0.64 ppm ozone for 8 hours a day (unpublished observations).

References

1. Lane BP, Gordon R: Regeneration of rat tracheal epithelium after mechanical injury: I. The relationship between mitotic activity and cellular differentiation. Proc Soc Exp Biol Med 1974, 145:1139-1144
2. Klein-Szanto AJP, Topping DC, Heckman CA, Nettesheim P: Ultrastructural characteristics of carcinogen-induced nondysplastic changes in tracheal epithelium. Am J Pathol 1980, 98:61-82
3. Harris CC, Sporn MB, Kaufman DG: Acute ultrastructural effects of benzo(a)pyrene and ferric oxide on hamster tracheobronchial epithelium. Cancer Res 1971, 31:1977-1989
4. Becci PJ, McDowell EM, Trump BF: The respiratory epithelium: IV. Histogenesis of epidermoid metaplasia and carcinoma in situ in the hamster. J Natl Cancer Inst 1978, 61:577-586
5. Barrett LA, McDowell EM, Hill TA, Pyeatte JC, Harris CC, Trump BF: Introduction of atypical squamous metaplasia with benzo(a)pyrene in cultured hamster tracheas Pathol Res Pract 1980, 168:134-145
6. Philpott DE, Harrison GA, Turnbill C, Black S: Ultrastructural changes in tracheal epithelial cells exposed to oxygen. Aviat Space Environ Med 1977, 48:812-818
7. Asmundson T, Kilburn KH, McKenzie WN: Injury and metaplasia of airway cells due to SO_2. Lab Invest 1973, 29:41-53
8. Boatman ES, Sato S, Frank R: Acute effects of ozone on cat lungs. Am Rev Respir Dis 1974, 110:157-169
9. Boatman ES, Frank R: Morphologic and ultrastructural changes in the lungs of animals during acute exposure to ozone. Chest 1974, 116:705-777
10. Schwartz LW, Dungworth DL, Mustafa MG, Tarkington BK, Tyler WS: Pulmonary responses of rats to ambient levels of ozone: Effects of 7-day intermittent or continuous exposure. Lab Invest 1976, 34:565-578
11. Mellick PW, Dungworth DL, Schwartz LW, Tyler WS: Short term morphologic effects of high ambient levels of ozone on lungs of rhesus monkeys. Lab Invest 1977, 36:82-90
12. Castleman WL, Tyler WS, Dungworth DL: Lesions in respiratory bronchioles and conducting airways of monkeys exposed to ambient levels of ozone. Exp Mol Pathol 1977, 26:384-400
13. Penha PD, Werthamer S: Pulmonary lesions by long term exposure to ozone. Arch Environ Health 1974, 29:282-289
14. Frasca JM, Auerback O, Parks VR, Jamieson JD: Electron microscopic observations of the bronchial epithelium of dogs: II. Smoking dogs. Exp Mol Pathol 1968, 9:380-399
15. Reznick-Schuller H, Reznick G, Mohr U: Effects of cigarette smoke on the bronchial epithelium of Syrian golden hamsters: Ultrastructural studies. J Natl Cancer Inst 1975, 55:353-355
16. Plopper CG, Mariassy AT, Wilson DW, Alley JL, Nishio S, Nettesheim P: Comparison of nonciliated tracheal epithelial cells in five mammalian species: Ultrastructure and population densities. Exp Lung Res 1983, 5:79-98
17. Wilson DW, Plopper CG, Hyde DM: The tracheobronchial epithelium of the bonnet monkey (Macaca radiata): A quantitative ultrastructural study. Am J Anat (In press)
18. Nowell JA, Pangborn J, Tyler WS: Stabilization and replication of soft tubular and alveolar systems: A scanning electron microscope study of the lung, Scanning Electron Microscopy/1972. Edited by Johari O, Corvin I. Chicago, Ill, IIT Research Institute, 1972, pp 305-13
19. Weibel ER: Stereologic Methods. Vol II. New York, Academic Press, 1980, pp 64-67
20. Ryan TA, Joiner BL, Ryan BF: Minitab Student Handbook. North Scituate, Mass, Duxbury Press, 1976, pp 134-215
21. Last JA, Jennings MD, Schwartz LW, Cross CE: Glycoprotein secretion by tracheal explants cultured from rats exposed to ozone. Am Rev Respir Dis 1977, 116:695-703
22. Wells AB: The kinetics of cell proliferation in the tracheobronchial epithelia of rats with and without chronic respiratory disease. Cell Tissue Kinet 1970, 3:185-206
23. Bindreiter M, Schuppler J, Stockinger L: Zellproliferation und differenzierung im trachealepithel der ratte. Exp Cell Res 1968, 50:377-382
24. Evans MJ, Cabral-Anderson LJ, Freeman G: Role of the Clara cell in renewal of the bronchiolar epithelium. Lab Invest 1978, 38:648-655
25. McDowell EM, Combs JW, Newkirk C: Changes in secretory cells of hamster tracheal epithelium in response to acute sublethal injury. Exp Lung Res 1983, 4:227-243
26. McDowell EM, Combs JW, Newkirk C: A quantitative light and electron microscopic study of hamster tracheal epithelium with special attention to so-called intermediate cells. Exp Lung Res 1983, 4:205-226
27. Castleman WL, Dungworth DL, Schwartz LW, Tyler WS: Acute respiratory bronchiolitis: An ultrastructural and autoradiographic study of epithelial cell injury and renewal in rhesus monkeys exposed to ozone. Am J Pathol 1980, 98:811-840
28. Breeze RG, Wheeldon EB: The cells of the pulmonary airways. Am Rev Respir Dis 1977, 116:705-777
29. Jeffrey PK, Reid L: New observations of rat airway epithelium: A quantitative and electron microscopic study. J Anat 1975, 120:295-320
30. McDowell EM, Barrett LA, Glavin F, Harris CC, Trump BF: The respiratory epithelium. I. Human bronchus. J Natl Cancer Inst 1978, 61:539-549
31. Keenan KP, Wilson TS, McDowell EM: Regeneration of hamster tracheal epithelium after mechanical injury. IV. Histochemical, immunocytochemical and ultrastructural studies. Virchows Arch [Cell Pathol] (in press)
32. Crapo JD, Barry BE, Foscue HA, Shelburne J: Structural and biochemical changes in rat lungs occurring during exposures to lethal and adaptive doses of oxygen. Am Rev Respir Dis 1980, 122:123-143